The Distribution of Congestion on a Class of Stochastic Kinematic Wave Model

Jorge A. Laval[a,*], Bhargava R. Chilukuri[a]

[a]*School of Civil and Environmental Engineering, Georgia Institute of Technology*

Abstract

This paper shows that a wide range of stochastic extensions of the kinematic wave model tend to the same parameter-free expression for the probability of congestion at a given time-space point. This is shown for white noise initial density with deterministic and stochastic fundamental diagram in the case of Riemann problems and the bottleneck problem. It is also found that the stochastic solution (i) preserves the structure of the deterministic solution, and (ii) tends to the deterministic solution with time at a given location.

Keywords: stochastic traffic flow, kinematic wave model

1. Introduction

Uncertainty is a key component in traffic flow modeling given measurement errors and random driver behavior. To the author's knowledge, existing research uses a numerical rather than analytical approach to account for uncertainty, generating random terms directly in the discrete model; see e.g. Sumalee et al. (2011) for the stochastic extension of the Cell Transmission model, Nagel and Schreckenberg (1992); Barlovic et al. (1998, 2002) for cellular automata models, Khoshyaran and Lebacque (2007) for second-order models, Helbing and Treiber (1998); Shvetsov and Helbing (1999); Helbing et al. (2001); Ngoduy et al. (2006); Ngoduy (2008) for gas-kinetic models, and Del Castillo (2001); Kim and Zhang (2008); Sopasakis (2004) for microscopic models.

*Corresponding author. Tel. : +1 (404) 894-2360; Fax : +1 (404) 894-2278

Email addresses: jorge.laval@ce.gatech.edu (Jorge A. Laval), bchilukuri3@gatech.edu (Bhargava R. Chilukuri)

This paper studies the kinematic wave model with (stochastic) triangular fundamental diagram and stochastic initial conditions, for which analytical solutions are possible. Closely related topics have attracted significant attention from mathematicians in the fields of conservation laws and Hamilton-Jacobi systems. In both cases the interest is the stochastic initial data and/or source term.

In the conservation law field (Avellaneda and Weinan, 1995; Burgers, 1974; Ryan, 1998; Sinai, 1992; Wehr and Xin, 1997; Antia and Basu, 2000; Dafermos, 2000; Holden and Risebro, 1993) uncertainty is incorporated only to Burgers' equation, which is a conservation law (eqn. (1) here) with flux function (fundamental diagram) equal to $F(k) = k^2/2$. They derive the solution of Burgers' equation using its variational formulation, known as the Lax-Olejnik (Lax, 1957; Olejnik, 1957) or the Hopf-Cole (Hopf, 1970) formula (eqn. (4) here). Apart from existence and uniqueness, the main result from the field is, according to the authors, that the probability distribution of the solution at any point in time-space can be expressed in terms of the solution at an arbitrary time when the initial data is a white noise. But since the flux function in traffic is nothing like Burger's and white noise initial data is not applicable to traffic flow, these results are not readily applicable in our case.

In the field of Hamilton-Jacobi equations (Barles and Souganidis, 2000; Benz, 2002; Rezakhanlou and Tarver, 2000; Rorro, 2006, 2005; Souganidis, 1999) much attention has been given to the problem of homogenization, which essentially states that small fluctuations in the initial data (stochastic or not) are averaged-out in such a way that the solution tends to the solution of a deterministic problem with a different fundamental diagram (i.e., the effective Hamiltonian). In all cases, however, the results are not directly transferable to traffic flow because it is always assumed that the flux function is convex and unbounded.

The link between conservation laws and Hamilton-Jacobi was brought up to the attention of the traffic flow theory community by Daganzo (2005a,b) who also unveiled important properties and solution methods. These references are the basis for the results presented in this paper, which is organized as follows. Section 2 presents a brief background on the kinematic wave model and its formulation as a Hamilton-Jacobi system. Section 3 defined the type of stochastic initial data used here, and Section 4 supplements this data with different variants of the bottleneck problem. Section 5 examines the stochastic the Riemann problem and shows that it has properties similar to the bottleneck problem. Finally, Section 6 presents a brief discussion.

2. Background

The kinematic wave model is a scalar conservation law of the vehicular density $k(t,x)$ at time t and location x, supplemented with initial or boundary data, and a fundamental diagram $F(t,x,k)$ that gives the flow $q(t,x)$ as a function of the local density:

$$\textbf{KW:} \begin{cases} k_t + F(k)_x = 0, & \text{(1a)} \\ k(t,x) = g(t,x), \quad \forall (t,x) \in \mathcal{B} & \text{(1b)} \end{cases}$$

where variables in subscript represent partial derivatives and $g(t,x)$ is a known function representing the density on a boundary $\mathcal{B}$. In terms of the vehicle number $N(t,x)$ the kinematic wave model becomes the Hamilton-Jacobi equation:

$$\textbf{HJ:} \begin{cases} N_t - F(-N_x) = 0, & \text{(2a)} \\ N(t,x) = G(t,x), \quad \forall (t,x) \in \mathcal{B} & \text{(2b)} \end{cases}$$

where $G(t,x)$ gives the data expressed in terms of vehicle number. Note that $k = -N_x$ and $q = N_t$. The solution of HJ equations can be expressed in variational form as:

$$N_P = \inf_{B \in \mathcal{B}_P} \{N_B + \Delta_{BP}\} \tag{3}$$

where P is a generic point with coordinates (t,x), $\mathcal{B}_P$ is the set of all points in the boundary that are in the domain of dependence of P, $B \equiv (t_B, x_B)$ is a point in $\mathcal{B}_P$, $N_P \equiv N(t,x)$ and $N_B \equiv N(t_B, x_B)$; see Fig. 1a. The term Δ_{BP} is the "cost" or maximum number of vehicles that can cross the line segment BP, which can be obtained by the integration of the maximum passing rate along the path BP:

$$\Delta_{BP} = \int_{t_B}^{t_P} R(t) dt \tag{4}$$

where $R(t)$ is the maximum passing rate along segment BP, or the Lagrangian in HJ theory. Hereafter, we suppose that the facility is homogenous and exhibits a triangular fundamental diagram:

$$F(k) = \min\{uk, (\kappa - k)w\} \tag{5}$$

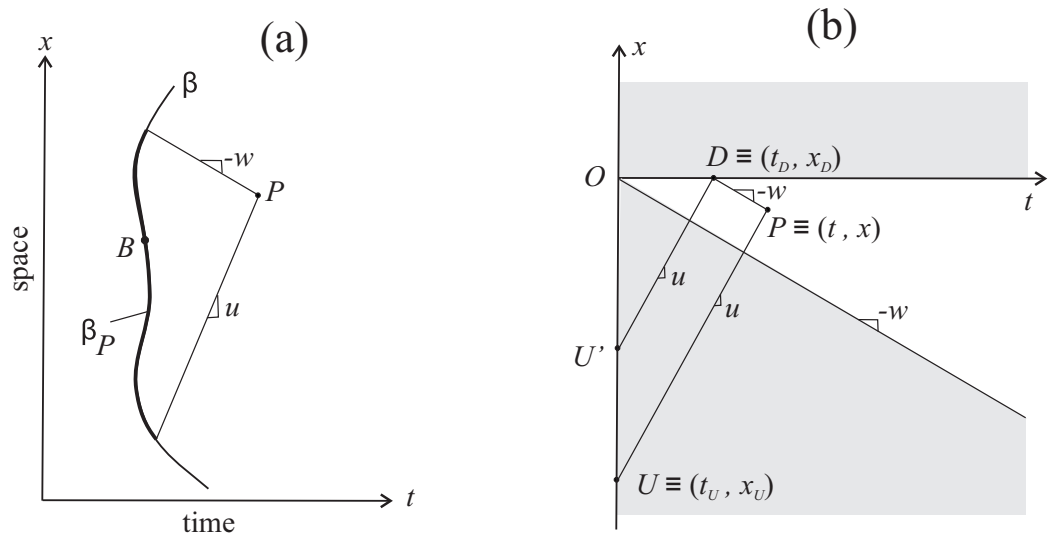

Figure 1: Basic definitions for (a) general variational problem, and (b) the bottleneck problem.

where u is the free-flow speed, $-w$ is the wave speed and κ is the jam density. Under this assumption, the maximum passing rate is $R(t) = Q - Kv(t)$, where $v(t)$ is the velocity of the vehicle. Thus, using (4) gives that the cost Δ_{BP} can be expressed as

$$\Delta_{BP} = (t - t_B)Q - (x - x_B)K \tag{6}$$

where $Q = uw\kappa/(u + w)$ and $K = Q/u$ are the capacity and critical density of the roadway, respectively. Daganzo (2005a) shows that if (i) the boundary between two points $U \equiv (t_U, x_U)$ and $D \equiv (t_D, x_D)$ is a straight line, and (ii) the density is constant between these points, then (3) becomes a linear program and thus its solution is determined by the boundary points only. Since the maximum passing rate for the upstream and downstream boundary points is 0 and κw, under these assumptions (3) simplifies to:

$$N_P = \min\{N_U; N_D + (x_D - x)\kappa\}. \tag{7}$$

For more details the reader is referred to Daganzo (2005a,b).

3. Stochastic initial data

In this paper we consider the stochastic initial value problem (SIVP) where the mean density at all locations at $t = 0$, $g(x)$, is given. We will further assume an additive random component; i.e.:

$$k(0, x) = g(x) + \sigma W'(x), \tag{8}$$

where $W'(x) = dW(x)/dx$ is a white noise in the sense that $\sigma W(x)$ is a Brownian motion with zero drift and variance rate σ^2 (in units of density). In terms of vehicle number the initial data can also be expressed as:

$$N(0, x) = G(x) - \sigma W(x), \qquad \text{with} \tag{9a}$$

$$G(x) = \int_x^{x_1} g(s)ds, \qquad x < x_1, \tag{9b}$$

where x_1 can be thought of as the position of the first vehicle on the road segment at $t = 0$, $N(x_1) = 0$ and $W(x_1) = 0$. It follows that $N(0, x)$ has the normal distribution with mean $G(x)$ and variance $\sigma^2(x_1 - x)$. More importantly, note that the difference in the vehicle number between two points on the boundary, $N(0, x_U) - N(0, x_D), x_D > x_U$, also has the normal distribution with mean $G(x_U) - G(x_D)$ and variance $\sigma^2(x_D - x_U)$.

3.1. Subcritical data

We say that stochastic initial data is subcritical if:

$$Pr(k(0, x) \geq K) \approx 0, \forall x \in x_U \leq x \leq x_D, \tag{10}$$

where $Pr(\cdot)$ stands for "probability". We conjecture here that (7) holds for subcritical stochastic data because of the following:

Lemma. For deterministic initial data $k(0, x) = g(x), x_U \leq x \leq x_D$ the number of candidate points minimizing (3) is reduced to the set of points $\{x_B\}$ satisfying $g(x_B) = K$ and $g'(x_B) < 0$, in addition to U and D.

Proof. Using t_B =0 and x=x_B in (6) and (9b) respectively, the term in brackets in (3) becomes $G(x_B) + tQ - (x - x_B)K$. The first and second order conditions for a minimum imply the result.$\Diamond$

Notice that a formal proof for the stochastic case is not needed for the purpose of this paper. Suffice it to say that in the rare circumstance that on a given realization $k(0, x) \geq K$ for some x, its contribution to N_B in (3), $k(0, x)dx$, is in fact null.

4. The bottleneck problem

In this section the subcritical SIVP is solved on a homogeneous segment with a single bottleneck of stationary capacity $\mu(t)$ located at $x = 0$, and:

$$g(x) = \begin{cases} (1+\alpha)\bar{\mu}/u & \text{if } x < 0, \\ 0 & \text{otherwise.} \end{cases}, -\infty < x < \infty, \tag{11}$$

where $\bar{\mu}$ is the mean bottleneck capacity, α is a dimensionless parameter such that $\alpha > 0$ ($\alpha < 0$) implies an initial density greater (lower) than the mean critical density at the bottleneck, $\bar{\mu}/u$. We are interested in the time-space points that are reachable by the bottleneck upstream of it; i.e., $0 \geq x \geq -wt$. Points downstream of the bottleneck are irrelevant in our problem because they will always be in free-flow. Accordingly, we note that point D is always at the bottleneck location and thus N_D is determined by either O or U'; see Fig. 1b. But if point D is in free-flow then $N_P = N_U$ since the initial data are subcritical, and therefore one can ignore point U' in the analysis altogether. Thus, we can apply (7) with $x_D = 0, N_D = N_0 + \Delta_{OD}$, which gives

$$N_P = \min\{N_U; \int_0^{t_D} \mu(t)dt - x\kappa\}, \tag{12}$$

after noting that $N_O = 0$ here. Our general procedure is as follows. For a given realization of all random variables and processes involved, the solution is always given by (12). This makes it possible to determine the "probability of congestion", $p(t, x)$, i.e. the probability that N_P is given by the downstream term:

$$p = Pr(\int_0^{t_D} \mu(t)dt - x\kappa < N_U). \tag{13}$$

It turns out that the contours $p(t, x) =$ constant can be expressed algebraically and thus are the main focus of the paper. Unfortunately, the mean and variance of N_P are not. To see this, notice that the distribution of N_P,

$$Pr(N_P > n) = Pr(N_U > n, \int_0^{t_D} \mu(t)dt - x\kappa > n), \tag{14}$$

involves the Bivariate Normal distribution, which can only be evaluated numerically.

Next, three scenarios are considered among combinations of random / deterministic bottleneck capacity and fundamental diagram.

4.1. Deterministic bottleneck capacity and fundamental diagram

Here we interpret $\bar{\mu} < Q$ as the deterministic bottleneck capacity. From (12) it follows that $N_P = \min\{N_U; \bar{\mu} t_D - x\kappa\}$ and the probability of congestion becomes:

$$p = \Phi(z), \qquad z = \frac{G(x_U) - \bar{\mu} t_D + x\kappa}{\sigma\sqrt{x_U}}, \tag{15}$$

where $\Phi(\cdot)$ is the cumulative standard normal distribution. Replacing $x_U = x - ut, t_D = t + x/w$ and $G(x_U) = -(1+\alpha)x_U\bar{\mu}/u$ gives

$$z(t,x) = \frac{(\kappa - \bar{\mu}\left((1+\alpha)/u + 1/w\right))\, x + \alpha\bar{\mu}t}{\sigma\sqrt{tu - x}}. \tag{16}$$

Despite the large number of parameters, this expression shows a universal shape using a suitable change of units, as shown next.

4.1.1. Relaxation time and dimensionless formulation

Much more information can be extracted from the standardized variable z by a suitable change of units that minimizes the number of parameters. To this end, we measure time in units of the "relaxation time", τ, defined in this paper as the time it takes to reach a given percentile z_α at $x = 0$; i.e., $z(\tau, 0) = z_\alpha$. Taking $z_\alpha = 1$ the rescaling constants are:

$$\tau = \frac{\sigma^2 u}{\alpha^2 \bar{\mu}^2}, \qquad \text{units of time} \tag{17a}$$

$$\xi = |s|\tau, \qquad \text{units of distance} \tag{17b}$$

where s can be interpreted as the slope of the shock arising in the deterministic solution when $\alpha > 0$; i.e.:

$$s = \frac{\alpha}{\kappa/\bar{\mu} - (1+\alpha)/u - 1/w}; \tag{18}$$

its interpretation when $\alpha < 0$ will be clear shortly. In this new dimensionless coordinate system

$$t' = t/\tau, \qquad x' = x/\xi, \tag{19}$$

one can express z in dimensionless form as follows, provided that $\alpha \neq 0$:

$$z'(t', x') = \frac{x' \pm t'}{\sqrt{t' - x'|s|/u}}, \tag{20}$$

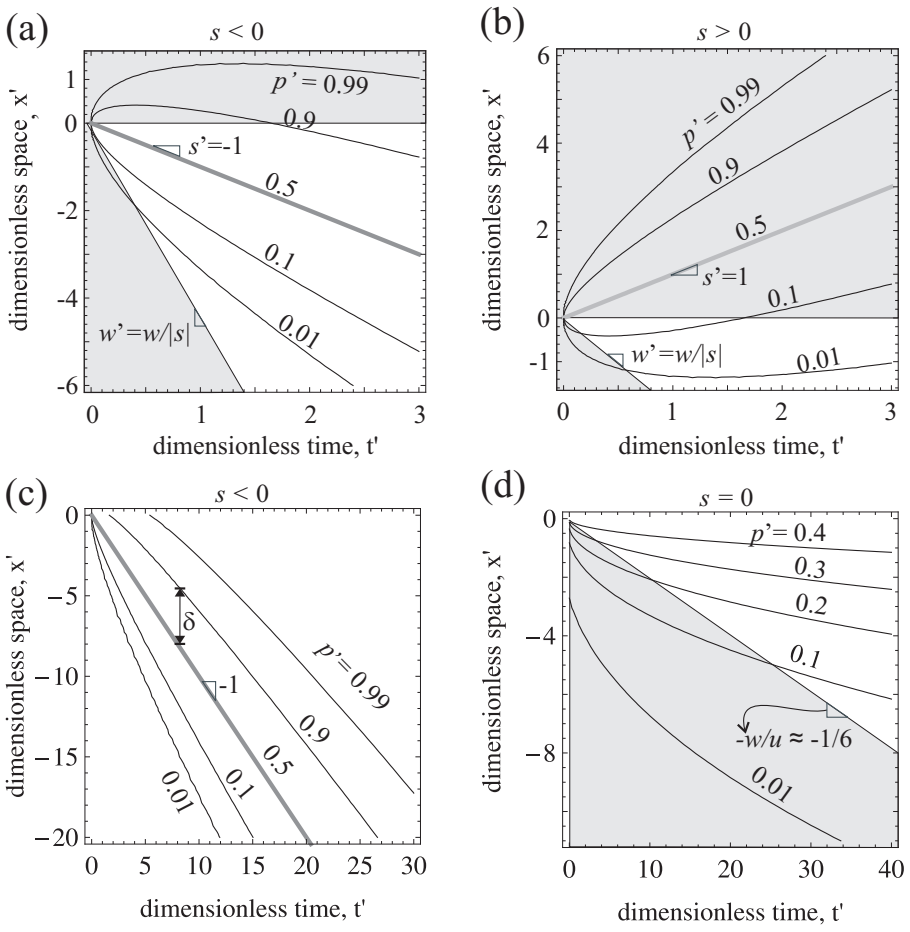

Figure 2: Contours of $p' = \Phi(z'(t', x'))$ with z' given by (21).

with $\pm$ given by $-\text{Sign}(s)$. For typical freeway problems $|s| \ll u$ and therefore (20) can be well approximated by

$$z'(t', x') = (x' \pm t')/\sqrt{t'} \tag{21}$$

Since (21) contains no parameters, it gives the universal shape for z. This means that $z(t, x)$ for various values of u, w, κ, σ, etc. differs from $z'(t', x')$ only by a change in units.

Figure 2a,b depict the contours of $p' = \Phi(z'(t', x'))$ for negative and positive shock speed, respectively. The gray areas in the figure indicate that (21) is not applicable in this particular case, as explained earlier. The

extent of these areas is determined by w given that rescaling (17) implies $x'/t' = (x/t)/|s|$ and thus speeds in the new system are measured in units of the shock speed, e.g. the new wave speed is $w' = w/|s|$ and the new shock speed is $s' =$Sign(s). It can be seen that both cases are mirror images of each other, that the different contours tend to follow the deterministic shock line, and that when the shock speed is positive the probability of congestion is significant (at most 0.5) on a bounded time-space region. This is not the case when $s < 0$, where this region is unbounded and contains all probabilities; see Fig. 2c.

When $\alpha = 0$ (and thus $s = 0$), (16) gives $z = (x\kappa(1 - \bar{\mu}/Q)/(\sigma\sqrt{tu - x})$, or in dimensionless form:

$$z'(t', x') = \frac{\sqrt{2}x'}{\sqrt{t' - x'}} \tag{22}$$

with rescaling $\tau = 2\sigma^2/(\kappa^2 u(1 - \bar{\mu}/Q)^2), \xi = u\tau$. It can be seen that at the bottleneck location $x' = 0$ the probability of congestion is one half, and that it decreases upstream of the bottleneck, as expected. This is illustrated in Fig. 2d. Notice that now the rescaling implies that speeds are measured in units of the free-flow speed and therefore the gray area in the figure is fixed, unlike previous cases.

4.2. Random bottleneck capacity and deterministic fundamental diagram

Here we generalize the bottleneck capacity in the previous section to be a random process:

$$\mu(t) = \bar{\mu} + \psi W'(t), \tag{23}$$

where ψ^2 is the variance rate (in units of flow). The key observations here are that (i) the maximum number of vehicles that can cross the bottleneck becomes a Brownian motion, and that (ii) this Brownian motion is independent of the demand. Therefore, the cost of path OD (e.g. in Fig. 1b) is a normal random variable with mean $\bar{\mu}t_D$ and variance $\psi^2 t_D$. It follows that:

$$p = \Phi(z), \quad z = \frac{G_U - \bar{\mu}t_D + x\kappa}{\sqrt{\sigma^2 x_U + \psi^2 t_D}}. \tag{24}$$

and in dimensionless form, provided that $\alpha \neq 0$:

$$z'(t', x') = \frac{x' \pm t'}{\sqrt{t' + \theta x'}}, \quad \theta = \frac{|s|}{w} \cdot \frac{\psi^2 - \sigma^2 w}{\psi^2 + \sigma^2 u}, \tag{25}$$

with rescaling as in (17) but now:

$$\tau = \frac{\psi^2 + \sigma^2 u}{\alpha^2 \bar{\mu}^2}. \tag{26}$$

Notice that θ is dimensionless. We argue that for typical problems θ can be neglected and therefore one can use (21) as a good approximation. This means that the main effect of bottleneck capacity being random is increasing the relaxation time by $\psi^2/(\alpha\bar{\mu})^2$, but that all other features remain arguably identical. To see why θ should be small, one can take a worst-case scenario with $|s| = w$ and a Poisson process for both initial values and bottleneck capacity (i.e. variance equal to the mean: $\sigma^2 = (1+\alpha)\bar{\mu}/u$, and $\psi^2 = \bar{\mu}$). This gives $\theta \approx 0.2$ for typical values $u/w \approx 6$ and $\alpha \approx 1$.

4.3. Random bottleneck capacity and fundamental diagram

The framework presented so far can accommodate random u, w and κ using standard probability theory. We illustrate this in the case of random bottleneck capacity in the previous section. The simplest way to accomplish this is to estimate the mean and variance for u, w^{-1}, κ and assume, reasonably, that these three random variables are all independent of each other. Using standard formulae for conditional expectation and conditional variance, it is straightforward to show that:

$$E[N_U] = (t\bar{u} - x)a \tag{27a}$$

$$E[N_D - x\kappa] = (t + x\overline{w^{-1}})\bar{\mu} - x\bar{\kappa} \tag{27b}$$

$$V[N_U] = (t\bar{u} - x)\sigma^2 + t^2\bar{\bar{u}}a^2 \tag{27c}$$

$$V[N_D - x\kappa] = (t + x\overline{w^{-1}})\psi^2 + (\bar{\mu}^2\overline{\overline{w^{-1}}} + \bar{\bar{\kappa}})x^2, \tag{27d}$$

where overbars and double overbars denote mean and variance, respectively, and $a = (1+\alpha)\bar{\mu}/\bar{u}$ denotes the mean initial density. It follows that the probability of congestion can be approximated by:

$$p = \Phi\left(\frac{E[N_U] - E[N_D - x\kappa]}{\sqrt{V[N_U] + V[N_D - x\kappa]}}\right). \tag{28}$$

The relaxation time

$$\tau = \frac{\psi^2 + \sigma^2\bar{u}}{(\alpha^2 - (1+\alpha)^2\bar{\bar{u}}/\bar{u}^2)\,\bar{\mu}^2} \tag{29}$$

coincides with (26) when the free-flow is deterministic, as expected. Interestingly, (29) is independent of both w and κ. This indicates that, as far as the fundamental diagram is concerned, the time to convergence to the deterministic solution is dictated by the free-flow speed only, and that the relationship is increasing with both $\bar{u}$ and the squared coefficient of variation $\bar{\bar{u}}/\bar{u}^2$. The latter is as expected because larger variability leads to larger relaxation times; note that $\sigma^2\bar{u}$ represents the variance rate at the bottleneck induced by the variance in the initial data.

Combining (28) and (29) does not yield a compact dimensionless representation; but the rescaling in the previous section does, and we obtain:

$$z'(t', x') = \frac{x' \pm t'}{\sqrt{t' + \theta x' + \theta_1 t'^2 + \theta_2 x'^2}}, \qquad \text{with:} \tag{30a}$$

$$\theta_1 = (1 + 1/\alpha)^2 \bar{\bar{u}}/\bar{u}^2, \tag{30b}$$

$$\theta_2 = \frac{s^2}{\alpha^2}\left(\bar{\bar{\kappa}}/\bar{\mu}^2 + \overline{\overline{w^{-1}}}\right), \tag{30c}$$

where s here is as in (18) but using mean values for u, κ and $1/w$; similarly for θ. This expression converges to (20) when the fundamental diagram is deterministic, as expected, which in turn converges to (21) as argued earlier. Fig. 3 shows the contours generated by (30) for three combinations of θ_1, θ_2 keeping $\theta = 0.03$, superimposed to the ones generated by (21), which requires no parameters. It can be seen that (21) provides a good approximation for small t', x' (say $t' < 10, x' > -5$) even with random fundamental diagrams. Indeed, the value for θ_1, θ_2 should stay within the ones considered in the figure in real application. To see this, it is well-known that free-flow branch of the fundamental diagram exhibits very little scatter, unlike the congested branch. Therefore, one expects the terms $\bar{\bar{u}}/\bar{u}^2$ and $\overline{\overline{w^{-1}}}$ to be small. Similarly, the variance in jam density should be mostly driven by the variance in vehicle sizes, which should be negligible compared with $\bar{\mu}^2$. Consideration shows that θ_1, θ_2 should be in the order of 10^{-2} and 10^{-1}, respectively.

5. Stochastic Riemann problems

Riemann problems are a special case of initial value problems and constitute the building block for developing Godunov-type numerical solution methods (Godunov, 1959; Daganzo, 1994), and also for solutions "by hand".

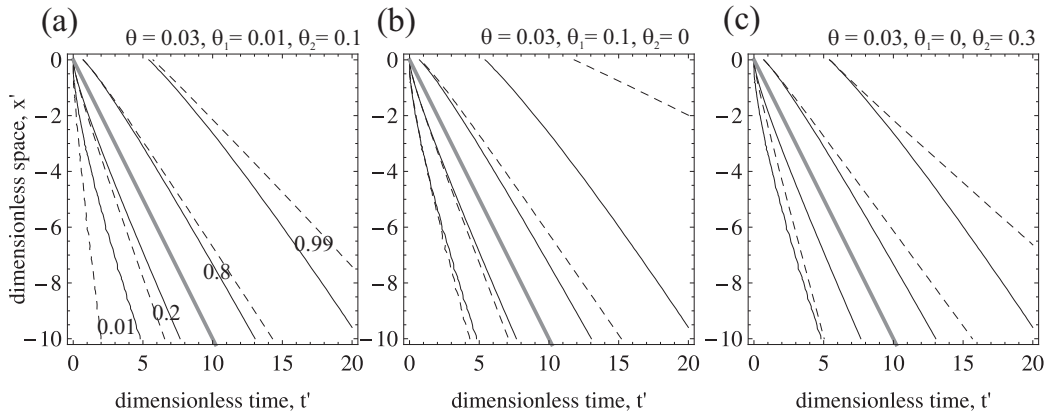

Figure 3: Contours of $p' = \Phi(z'(t', x'))$ with z' given by (30) in dashed lines superimposed to the ones given by (21) in solid lines.

Here we consider a deterministic fundamental diagram and initial values given by (8) with

$$g(x) = \begin{cases} k_U & \text{if } x < 0, \\ k_D & \text{otherwise.} \end{cases} , -\infty < x < \infty; \tag{31}$$

see Fig. 4a. We are interested in (i) non-trivial problems where the discontinuity at the origin contains the critical density K, and (ii) the time-space points that are reachable from the origin; i.e., $-wt \leq x \leq ut$; see Fig. 4b. Recall that in the deterministic case there are two possible solutions: (i) the deceleration or shock solution when $k_U < K < k_D$, and (ii) the acceleration or rarefaction fan solution when $k_U > K > k_D$. Note also that the Lemma implies that the deceleration solution has only two candidates (because $g'(0) = +\infty$ is positive), and the acceleration solution, three. For maximum generality, we consider all three candidates for both solutions in what follows, i.e.:

$$N_P = \min\{N_U; N_O + tQ - xK; N_D + (x_D - x)\kappa\}. \tag{32}$$

Let p_U, p_O, p_D be the probability of each one of these candidates to be the minimum. To determine these probabilities, we note that the change in the number of vehicles between DO and OU are independent by virtue of Brownian motions' independent increments property. Therefore, $p_O = Pr(N_O + tQ - xK < N_U)Pr(N_O + tQ - xK < N_D + (x_D - x)\kappa)$, which will

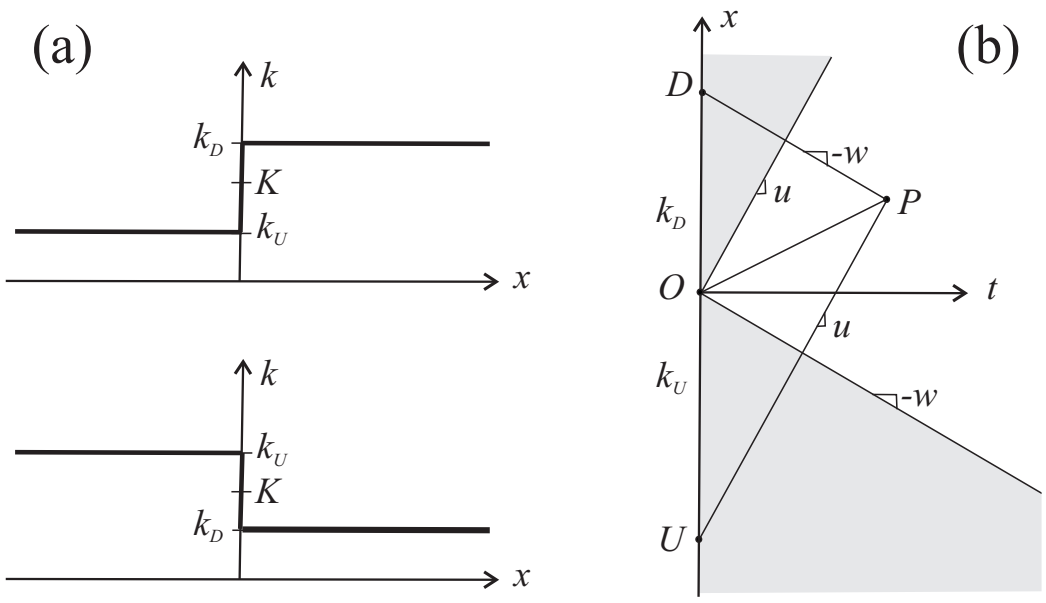

Figure 4: Stochastic Riemann problems: (a) deterministic component initial values, $g(x)$; (b) time-space points involved.

be simplified momentarily. Let $D|\bar{O}$ denote the event that the minimum of (32) comes from D given that it does not come from O. Then, the probability that N_P is given by the downstream term is $p_{D|\bar{O}} = Pr(N_D+(x_D-x)\kappa < N_U)$. Noting that the difference in vehicle number between two candidates are also normally distributed, after some manipulations one can show that:

$$p_O = \Phi(z_{OU})\Phi(z_{OD}) \tag{33a}$$

$$p_{D|\bar{O}} = \Phi(z_{DU}) \tag{33b}$$

$$p_D = (1 - p_O)p_{D|\bar{O}} \tag{33c}$$

$$p_U = (1 - p_O)(1 - p_{D|\bar{O}}) \tag{33d}$$

and

$$z_{DU}(t, x) = \frac{(k_U - k_D)(st - x)}{\sigma\sqrt{t(u + w)}} \tag{34a}$$

$$z_{OU}(t, x) = \sqrt{ut - x}\,(k_U - K)\,/\sigma \tag{34b}$$

$$z_{OD}(t, x) = \sqrt{wt + x}\,(K - k_D)\,/\sigma \tag{34c}$$

are standardized variables. The standardized variables z_{OU} and z_{OD} (i) are negative (positive) in the deceleration (acceleration) solution, (ii) tend to $-\infty$ ($+\infty$) at a rate proportional to $\sqrt{t}$ for fixed x, (iii) this rate decreases with the variability parameter σ, and (iv) they vanish along the lines $x = ut$ and $x = -wt$, respectively. The variable z_{DU} shares the same properties above, except that its sign changes when crossing the line $x = st$, where it vanishes. This means that the shock solution for deterministic deceleration problems corresponds to the 50th percentile solution in the stochastic problem, as in section 4.

From (i) above and (33a) we see that for deceleration problems the probability p_O should become small very quickly with time because it is the product of two numbers that tend to zero rather quickly. Conversely, for acceleration problems this probability quickly tends to one. This means that the stochastic solution tends to the deterministic solution for large enough t, again, as in section 4. Interestingly, it turns out that the deceleration problem converges much more quickly than the acceleration problem (in the order of five times more rapidly for typical values). Although not proven here, this is a consequence of the Normal probability density function being symmetric and $\Phi(z) < 1$.

Finally, a dimensionless formulation cannot be achieved with the same rescaling for all three standardized variables. Interestingly, in the case of z_{DU} the relaxation time is $\tau = (u + w)\sigma^2/((k_D - k_U)^2 s^2)$ and one obtains (21) once again. This indicates that all problems analyzed in section 4 behave as the shock solution of stochastic Riemann problems.

6. Discussion

We have shown that different stochastic variants of the kinematic wave model with triangular fundamental diagram tend to the same parameter-free expression (21), which corresponds to the shock solution of stochastic Riemann problems. The main difference in the solution of all these variants is the relaxation time, which increases with the "amount of variance" in each case. In all cases the probability of congestion is 0.5 along the deterministic shock trajectory. But this shock has a width, $\delta(t', z_1)$, in the stochastic setting, which depends on the target percentile z_1; see Fig. 2c ($\Phi(z_1) = 0.9$ in the figure). It is straightforward to show that:

$$\delta(t', z_1) = 2|z_1|\sqrt{t'}, \tag{35}$$

which grows at a rate that tends to zero. It follows that the probability contours travel in the direction of the shock, shying away from it but at a rate that tends to zero. This indicates that for large t' these contours tend to become parallel to each other (and to the deterministic shock), and thus the deterministic structure tends to be preserved in the stochastic setting.

Another alternative to include variability in the fundamental diagram is to consider paths UP, DP as Brownian motions, as suggested by Newell (2002) in the case DP. Consideration shows that the main insight from section 4.3 remains valid in this case as well. This is because the variance of a Brownian motion increases linearly in time and therefore θ_1, θ_2 are identically zero in (30).

References

Antia, H., Basu, S., 2000. Temporal variations of the rotation rate in the solar interior. Astrophys. J. 541, 442–448.

Avellaneda, M., Weinan, E., 1995. Statistical properties of shocks in burgers turbulence. Communications in Mathematical Physics 172, 13–38.

Barles, G., Souganidis, P., 2000. On the large time behavior of solutions of hamilton-jacobi equations. SIAM Journal on Mathematical Analysis 31 (4), 925 – 939.

Barlovic, R., Huisinga, T., Schadschneider, A., Schreckenberg, M., 2002. Open boudaries in a cellular automaton model for traffic flow with mtastable states. Physical Review E 66, 1–11.

Barlovic, R., Santen, L., Schadschneider, A., Schreckenberg, M., 1998. Metastable states in cellular automata for traffic flow. The European Physical Journal B 5, 793–800.

Benz, A., 2002. Plasma Astrophysics: Kinetic Processes in Solar and Stellar Coronae, 2nd Edition. Vol. 279 of Astrophysics and Space Science Library. Kluwer, Dordrecht, Netherlands; Boston, U.S.A.

Burgers, J. M., 1974. The nonlinear diffusion equation : asymptotic solutions and statistical problems. D. Reidel Pub. Co., Dordrecht-Holland; Boston.

Dafermos, C. M., 2000. Hyperbolic conservation laws in continuum physics. Springer, Berlin; New York.

Daganzo, C. F., 1994. The cell transmission model: A dynamic representation of highway traffic consistent with the hydrodynamic theory. Transportation Research Part B 28 (4), 269–287.

Daganzo, C. F., 2005a. A variational formulation of kinematic wave theory: basic theory and complex boundary conditions. Transportation Research Part B 39 (2), 187–196.

Daganzo, C. F., 2005b. A variational formulation of kinematic waves: Solution methods. Transportation Research Part B: Methodological 39 (10), 934 – 950.

Del Castillo, J. M., 2001. Propagation of perturbations in dense traffic flow: a model and its implications. Transportation Research Part B 35 (2), 367–390.

Godunov, S., 1959. A difference scheme for numerical computation of discontinuous solutions of equations of fluid dynamics. Mat. Sb. 89 (47), 271–306.

Helbing, D., Hennecke, A., Shvetsov, V., Treiber, M., 2001. Master: Macroscopic traffic simuation based on a gas-kinetic, non-local traffic model. Transportation Research Part B 35, 183–211.

Helbing, D., Treiber, M., 1998. Gas-kinetic-based traffic model explaining observed hysteresis phase transition. Physical Review Letters 81, 3042–3045.

Holden, H., Risebro, N. H., 1993. Conservation laws with a random source. Inst., Univ., Oslo.

Hopf, E., 1970. On the right weak solution of the cauchy problem for a quasilinear equation of first order. Indiana Univ. Math. J. 19, 483–487.

Khoshyaran, M., Lebacque, P., 2007. A stochastic macroscopic traffic model devoid of diffusion. In: Traffic and Granular Flow '07.

Kim, T., Zhang, H. M., 2008. A stochastic wave propagation model. Transportation Research Part B 42, 619–634.

Lax, P. D., 1957. Hyperbolic systems of conservation laws ii. In: Sarnak, P., Majda, A. (Eds.), Communications on Pure and Applied Mathematics. Wiley Periodicals, p. 537566.

Nagel, K., Schreckenberg, M., 1992. A cellular automaton model for freeway traffic. Journal of Physics I 2 (2), 2221 – 2229.

Newell, G. F., 2002. A simplified car-following theory : a lower order model. Transportation Research Part B 36 (3), 195–205.

Ngoduy, D., 2008. Operational effect of acceleration lane on main traffic flow at disconituities. Transportmetrica 4, 195–207.

Ngoduy, D., Hoogendoorn, S., Van Zuylen, H., 2006. New continuum traffic model for freeway with on- and off-ramp to explain different traffic congested states. Transportation Research Record 1962, 92–102.

Olejnik, O., 1957. Discontinuous solutions of non-linear differential equations. translated by george biriuk. Am. Math. Soc., Transl., II. Ser. 26, 95–172.

Rezakhanlou, F., Tarver, J. E., 2000. Homogenization forstochastic hamilton-jacobi equations. Archive for Rational Mechanics and Analysis 151, 277–309.

Rorro, M., 2005. Numerical approximation of the effective Hamiltonian and of the Aubry set for first order Hamilton-Jacobi equations. Proceedings of Science SISSA cstna2005-016.

Rorro, M., 2006. An approximation scheme for the effective hamiltonian and applications. Applied Numerical Mathematics 56 (9), 1238 – 1254, numerical Methods for Viscosity Solutions and Applications.

Ryan, R., 1998. Large-deviation analysis of burgers turbulence with white-noise initial data. Communications on Pure and Applied Mathematics 51 (1), 47–75.

Shvetsov, V., Helbing, D., 1999. Macroscopic dynamics of multilane traffic. Physical Review E 59, 6328–6339.

Sinai, Y., 1992. Statistics of shocks in solutions of inviscid burgers equation. Communications in Mathematical Physics 148, 601–621.

Sopasakis, A., 2004. Stochastic noise approach to traffic flow modeling. Physica A: Statistical Mechanics and its Applications 342 (3-4), 741 – 754.

433 Souganidis, P. E., 1999. Stochastic homogenization of hamiltonjacobi equa-
434 tions and some applications. Asymptotic Analysis 20 (1), 1 – 11.

435 Sumalee, A., Zhong, R., Pan, T., Szeto, W., 2011. Stochastic cell transmis-
436 sion model (sctm): A stochastic dynamic traffic model for traffic state
437 surveillance and assignment. Transportation Research Part B: Method-
438 ological 45 (3), 507 – 533.

439 Wehr, J., Xin, J., 1997. Front speed in the burgers equation with a random
440 flux. Journal of Statistical Physics 88, 843–871.